Journal of the European Ceramic Society 22 (2002) 661–671

www.elsevier.com/locate/jeurceramsoc

Phase stability of $SrFeCo_{0.5}O_y$ under synthesis and annealing conditions

B.J. Mitchell[a], J.W. Richardson Jr.[a,*], C.D. Murphy[a], B. Ma[b], U. Balachandran[b], J.P. Hodges[c], J.D. Jorgensen[c]

[a]*Intense Pulsed Neutron Source, Argonne National Laboratory, Argonne, IL 60439, USA*
[b]*Energy Technology Division, Argonne National Laboratory, Argonne, IL 60439, USA*
[c]*Materials Science Division, Argonne National Laboratory, Argonne, IL 60439, USA*

Received 13 October 1999; received in revised form 29 April 2001; accepted 20 May 2001

Abstract

Dense ceramic tubes of the multi phase mixed ionic/electronic conductor $SrFeCo_{0.5}O_y$ (SFC2) have been .synthesized by solid-state reaction. Stability of the component phases of SFC2 was studied by insitu neutron diffraction in the temperature range of 900–1200 °C in air and Ar environments. In air between 900 and 1050 °C, the material is stable, with $Sr_2(Fe,Co)_3O_y$ (236) being the major phase. Above 1050 °C, 236 undergoes decomposition into perovskite and rocksalt phases, and at 1200 °C, only a small fraction of the 236 phase is stable. In Ar, the 236 phase is completely stable at 900 °C but is completely decomposed by 1100 °C, whereupon only the perovskite and rocksalt phases remain. Rietveld analysis indicates that the 236 and perovskite phases become more Fe-rich as decomposition occurs, while the perovskite phase lattice parameter and oxygen content vary readily as temperature and gas environment are changed. © 2002 Published by Elsevier Science Ltd.

Keywords: Membranes; Neutron diffraction; Phase composition; Stability; $SrFeCo_{0.5}O_y$

1. Introduction

Recently, the mixed-conducting oxide $SrFeCo_{0.5}O_y$ (SFC2) has been identified as a potential dense ceramic membrane that can be used to separate gas at elevated temperatures. Indeed, Balachandran et al.[1] demonstrated that extruded membrane tubes of SFC2 can be used for partial oxidation of methane to produce syngas ($CO + H_2$) in a methane conversion reactor operating at ~850 °C. The oxygen flux obtained from the separation of air in this reactor is commercially feasible, and the use of this technology could significantly reduce the cost of oxygen separation.[2]

Ceramic oxides have been considered for membrane applications for many years. Teraoka et al.[3,4] initially showed that certain ceramic materials, including some perovskite-based oxides, exhibit oxygen permeability at high temperatures while remaining impenetrable to other gases. Typically, $ABO_{3-\delta}$ perovskite materials[5–8] have been studied for oxygen diffusion properties or membrane applications, and, as-synthesized, these are single-phase materials. SFC2 is different from the $ABO_{3-\delta}$ perovskites in that it is not a single-phase material under standard synthesis conditions. Four known[9,10] phases, $Sr_2Fe_{3-a}Co_aO_{6.5-\delta}$ (236), $SrFe_{1-b}Co_bO_{3-\delta'}$ (perovskite/brownmillente), $Co_{3-c}Fe_cO_3$ (rock salt), and $Co_{3-d}Fe_dO_4$ (spinel), are certainly identifiable; with their presence dependent upon synthesis conditions. Guggilla and Manthiram[11] and Ma et al.[12] have shown that substitution of Co for Fe in $SrFe_{1.5-x}Co_xO_y$ produces single-phase materials only over a limited Co range. This finding suggests that Co^{3+} is not particularly stable within the 236 phase. The enhanced performance of SFC2 relative to that of the individual phases, as reported by Ma et al.,[12] is not yet understood.

The layered structure of $Sr_2(Fe,Co)_3O_{6.5-\delta}$ (see Fig. 1) is formed from perovskite and double-layer intergrowths. The Fe/Co atoms are assumed to be in +3 oxidation state and occupy three distinct environments: octahedral (6-fold), trigonal bi-pyramidal (distorted 5-fold), and square pyramidal (distorted 5-fold). The

* Corresponding author.
E-mail address: jwrichardson@anl.gov (J.W. Richardson Jr.).

0955-2219/02/$ - see front matter © 2002 Published by Elsevier Science Ltd.
PII: S0955-2219(01)00367-3

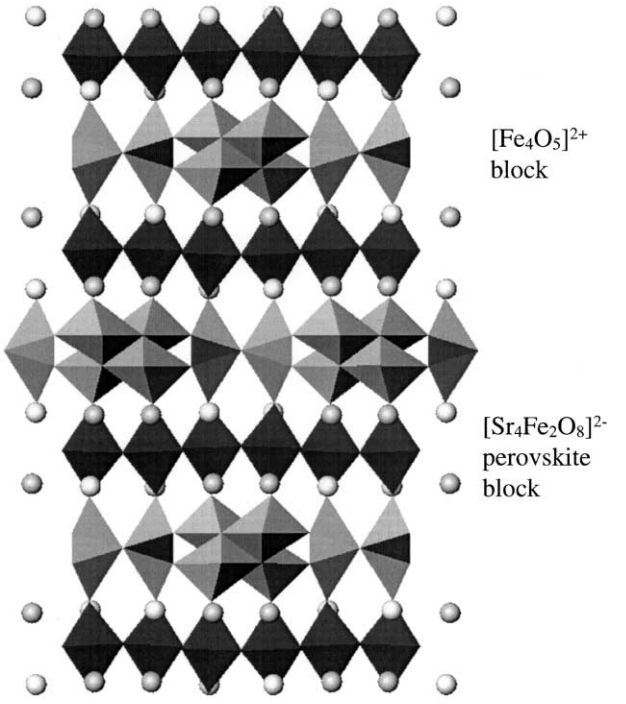

Fig. 1. Crystal structure of $Sr_2Fe_3O_{6.5-\delta}$, showing layered structure comprised of perovskite and double-layer blocks.

reported orthorhombic structure of 236 (space group Iba2) is related to the basic perovskite cell by the relationships $a=2\sqrt{2}a_p$, $b\sim5a_p$, $c=\sqrt{2}a_p$.

Fig. 2 shows the crystal structure of $Sr(Fe,Co)O_{3-\delta}$ perovskite (Pm–3m space group) and the defect ordered $Sr_2(Fe,Co)_2O_5$ (Ibm2 space group shown) brownmillente. In the perovskite structure six oxygen atoms form regular octahedra surrounding the Fe/Co atoms. The structure can readily adopt nonstoichiometry in the oxygen sub lattice, with oxygen vacancies formed randomly or in an ordered manner. Brownmillerite has a supercell ordering of vacancies with a relationship to the perovskite structure given by $a=\sqrt{2}a_p$, $b=4a_p$, $c=\sqrt{2}a_p$. Layers of corner sharing $(Fe,Co)O_6$ octahedra alternate along b with $(Fe,Co)O_4$ distorted tetrahedra. These ordered vacancies can be disordered at high temperature, where the material adopts the disordered perovskite structure.

Although as-synthesized (air annealed) SFC2 is known to contain four phases, the phase compositions of SFC2 samples annealed in different oxygen atmospheres are not known. Ambient-temperature neutron diffraction (ND) measurements on SFC2, annealed at 1100 °C under N_2, reveal a two-phase mixture, the phases being the vacancy-ordered brownmillerite $Sr_2(Fe,Co)_2O_5$ (Icmm space group used in Rietveld refinement) and (Co,Fe)O rocksalt (Fm–3m space group). The space group Ibm2 was found by Von-Harder and Muller-Buschbaum[13] to be correct for a single crystal of $Sr_2Fe_2O_5$. We find on powder samples, though, that the higher symmetry Icmm space group reported by

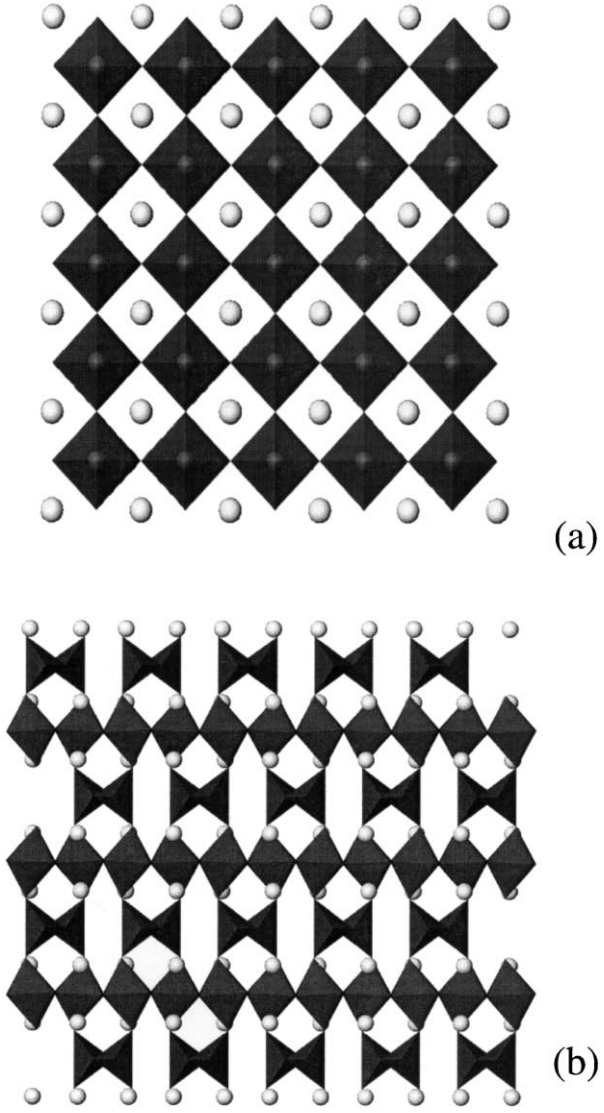

Fig. 2. Crystal structures of (a) $Sr(Fe,Co)O_{3-\delta}$ perovskite and (b) $Sr_2(Fe,Co)_2O_5$ brownmillerite.

Greaves et al.[14] provides a more satisfactory fit to the data, in agreement with other studies performed on powder samples.[15,16]

A more complete study is clearly required in order to determine how phase fractions of individual phases vary as a function of temperature and annealing environment, since alternative post-annealing treatments may produce ceramic membranes with improved performance and long-term stability. No studies of phase stability in SFC2 over a wide range of temperatures of oxygen partial pressures (pO_2) have been reported. During membrane manufacture, the sintering stage must be performed at high temperature to produce very dense ceramics, but annealing conditions could potentially be adjusted to improve performance. Neutron diffraction offers advantages over X-ray diffraction (XRD) for studying phase composition changes in Sr $(Fe,Co)_{1.5}O_y$ membrane materials, because neutron coherent scattering lengths

are not proportional to the atomic weights of constituent elements (significantly different for the elements here), and because oxygen can readily be detected within structures containing heavier atoms. Furthermore, neutrons, with their high penetrating power, allow the use of standard-thickness tubes. Finally, at a pulsed spallation neutron source, the entire diffraction pattern is measured simultaneously at every scattering angle, and scattering from furnace components and special environment furnace sample holders (made of alumina) is not seen by detectors in 90° scattering geometry. In this paper we present results from in situ ND measurements made on SFC2 membrane tubes over the temperature range of 900–1200 °C in both air and Ar environments, these being two possible synthesis and post-annealing conditions in the manufacture of SFC2 membranes.

2. Experimental

$SrFeCo_{0.5}O_y$ powder was prepared by a solid-state reaction of appropriate amounts of $SrCO_3$, $Co(NO_3)_2 \cdot 6H_2O$ and Fe_2O_3. Mixing and grinding were conducted for 10 h in iso-propanol with zirconia media. After drying, the mixture was calcined in air at 850 °C for 16 h, with intermittent grinding. After the final calcination, the powders were ground to an average particle size of ~ 7 μm. The resulting finely divided powder was packed into a mold and isostatically pressed with a 30,000 psi load. The green-body tube was removed from the mold and sintered in air for 5 h at 1200 °C at a heating rate of 120 °C·h^{-1} and cooling rate of ~ 90 °C·h^{-1}. These sintered tubes have a wall thickness of ~ 0.9 mm and their bulk density is $> 90\%$ of theoretical density.

Neutron diffraction measurements were carried out on the general purpose powder diffractometer (GPPD) at the intense pulsed neutron source (IPNS) at Argonne National Laboratory. Measurements were performed with a controlled atmosphere "Miller" furnace, over the temperature range of 900–1200 °C under flowing air (AGA < 10 ppm H_2O) and Ar (AGA 99.996%, pO_2 $\sim 10^{-5}$ atm). The furnace was heated/cooled at 240 °C·h^{-1} and allowed a 20-mm equilibration period at temperature. Gas flows were controlled with Brooks Series 5820 mass flow controllers. Data were collected at 15-, 30-, or 60-min intervals on the 90° banks, and Rietveld analysis was performed with GSAS.[17] The data were fitted with a model that assumed the presence of 236, perovskite, and rocksalt phases. Individual phase peak widths were obtained from a summed 1050 °C data set (6 h); no evidence of broadening was detected. For individual short runs, in addition to background and histogram scale factors, only lattice parameters and phase fractions were allowed to vary. We found that when we summed consecutive data sets in regions of phase composition stability (to improve counting statistics), it was possible to refine other parameters as described below.

In all of these experiments, the fabricated membrane tubes were initially heated to 1050 °C for a period of 8 h to ensure removal of any spinel phase that may have been formed in the cooling process during tube synthesis. This time period also allows the phases to reach reasonably stable levels, before they are cooled/heated to the appropriate temperature. In the first of three experiments, the sample was cooled from 1050 to 900 °C and measurements were made in air and Ar. In experiment 2, the sample was initially cooled from 1050 to 950 °C and measurements made in air and Ar at progressively higher temperatures, following the sequence shown in Table 1. In experiment 3, the sample was heated from 1050 to 1200 °C and measurements made in air and Ar, following the sequence shown in Table 2.

Neutron diffraction beamtime limitations restricted the available counting time for each state (temperature and gas environment), so in many cases the system may not have attained thermodynamic equilibrium. To efficiently use the experimental time, measurements were stopped when phase fractions had stabilized or rates of change were significantly diminished. Fig. 3 demonstrates this strategy in action. In this sequence from experiment 2, after measurements in air at 1050 and 950 °C, and a series of measurements at 950 °C in Ar, the furnace was heated to 1000 °C and the carrier gas switched to air immediately at the conclusion of the final 950 °C Ar run. Where possible, consecutive data sets in regions of minimal change were summed, and,

Table 1
Measurement sequence performed on SFC2 sample in experiment 2

Temperature (°C)	Measurement (air)	Number (Argon)
950	1	2
1000	3	4
1050	5	6
1100	7	
1150	8	

Table 2
Measurement sequence performed on SFC2 sample in experiment 3

Temperature (°C)	Measurement (air)	Number (Argon)
1050	1	
1200	2	3
1200	4	5
1100		6
1000		7
900		8
700		9
500		10
850		11

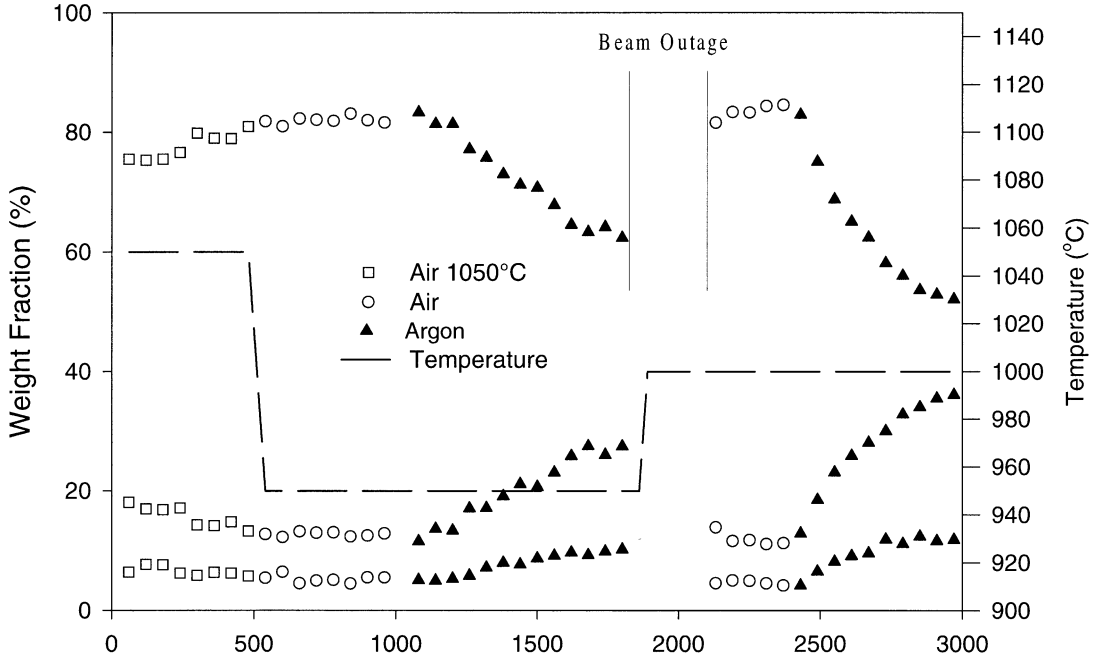

Fig. 3. Variation in weight fractions of (top) 236, (center) perovskite, and (bottom) rock salt phases in air and Ar at 950–1050 °C. A ~2 h period of beam outage is marked on the figure.

with the resultant improved counting statistics, oxygen content and Fe:Co ratios reliably refined.

3. Results and discussion

3.1. Ambient diffraction measurements

Ambient XRD and ND studies of SFC2 materials prove to be rather challenging, particularly because there is usually considerable strain broadening in the 236 and perovskite phases when samples have been air annealed and cooled by normal means. The strain can be relieved at a few hundred degrees Celsius—recognizable as a sharpening of diffraction peaks—where peak shape profile parameters reach values approaching instrumental resolution. Unless samples have been rapidly cooled/quenched from high temperature, some conversion of the $(Co,Fe)_3O_3$ rocksalt phase to the more complex $(Co,Fe)_3O_4$ spinel phase occurs. This can be reversed, but only at temperatures above 900 °C.[9] Another complication for ND is the presence of 236 reflections that are magnetic in origin. Asti et al.[18] found that $Sr_7Fe_{10}O_{22}$ was antiferromagnetic below a Ned temperature T_N ~50 °C. $Sr_2Fe_3O_{6.5-\delta}$ is believed to be isostructural with $Sr_7Fe_{10}O_{22}$ (i.e. part of a solid solution) and at room temperature shows magnetic reflections that disappear at elevated temperatures. Rietveld refinements of room temperature data obtained from laboratory XRD instrumentation seem adequate in terms of the fitting of individual phases, but refinements with the corresponding ND data are not. For these reasons, neutron diffraction data at elevated temperature were used as the basis for developing a standard model for subsequent refinements.

Rietveld refinements with synchrotron and neutron powder diffraction data from the single-phase Fe end member 236 phase, $Sr,Fe_3O_{6.5-\delta}$, indicate that the structure is incorrect, at least in terms of its space group. Fits to neutron and synchrotron X-ray data are shown in Figs. 4 and 5, respectively. The prominence of reflections defying the I-centering condition of the proposed space group (see Figs. 4 and 5) is a strong indication of a dramatic departure from the presumed symmetry. From both sets of data, it is the double-layer block within the 236 structure (see Fig. 1 for identification) that presents most difficulties, with excessively large thermal parameters and instability of positional parameters. Refinements of high resolution ND data collected above the Néel temperature showed no evidence of a phase change (although the magnetic reflections were gone) and continued to exhibit significant instability, again suggesting that the space group designation is incorrect. Efforts to resolve these discrepancies are continuing, but have so far been unsuccessful. Although the Fe end member clearly presents severe problems with the structure of $Sr_4Fe_6O_{13}$ described by Yoshiasa et al.,[19] these problems are much less significant for Co-doped samples as found in SFC2. Until the correct cell and space group are correctly determined, the Iba2 space group is sufficient for use in studies of 236 in multiple phase SFC2 as demonstrated by Fjellvag et al.[20] We have used the Yoshiasa structure to fit the 236 phase in SFC2.

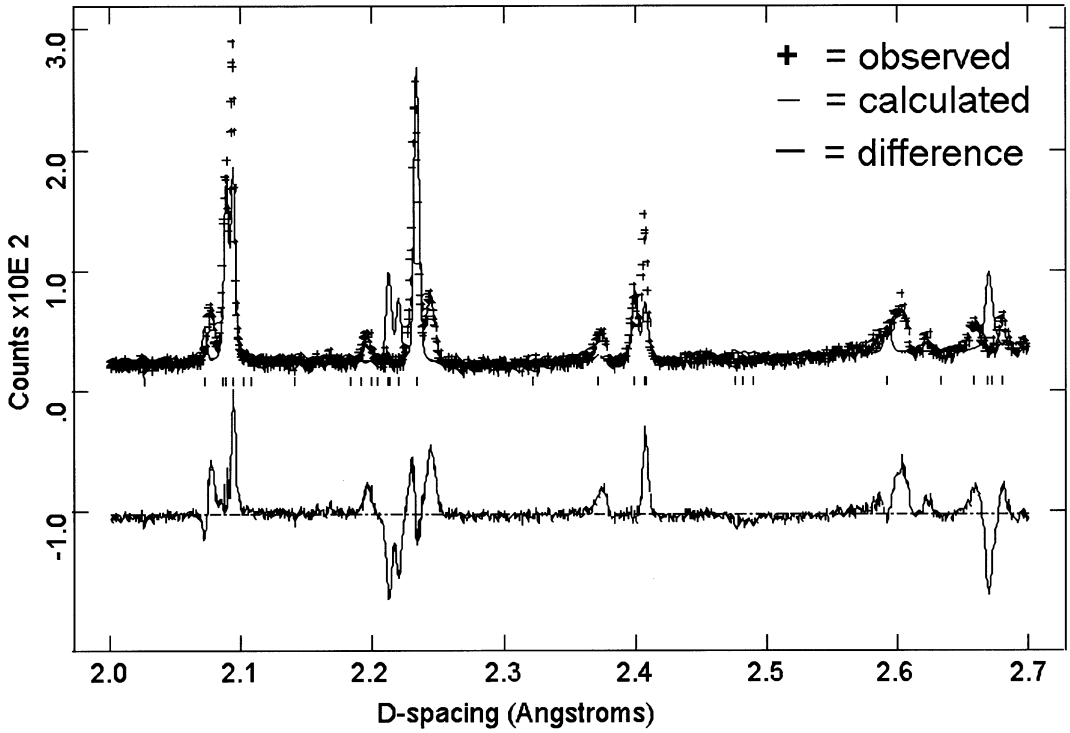

Fig. 4. Rietveld profile fit to ND data from $Sr_2Fe_3O_{65-\delta}$ sample. Observed (+), calculated, and difference profiles are shown, along with reflection markers. Note reflection at $d = 2.24$ Å which violates I-centering.

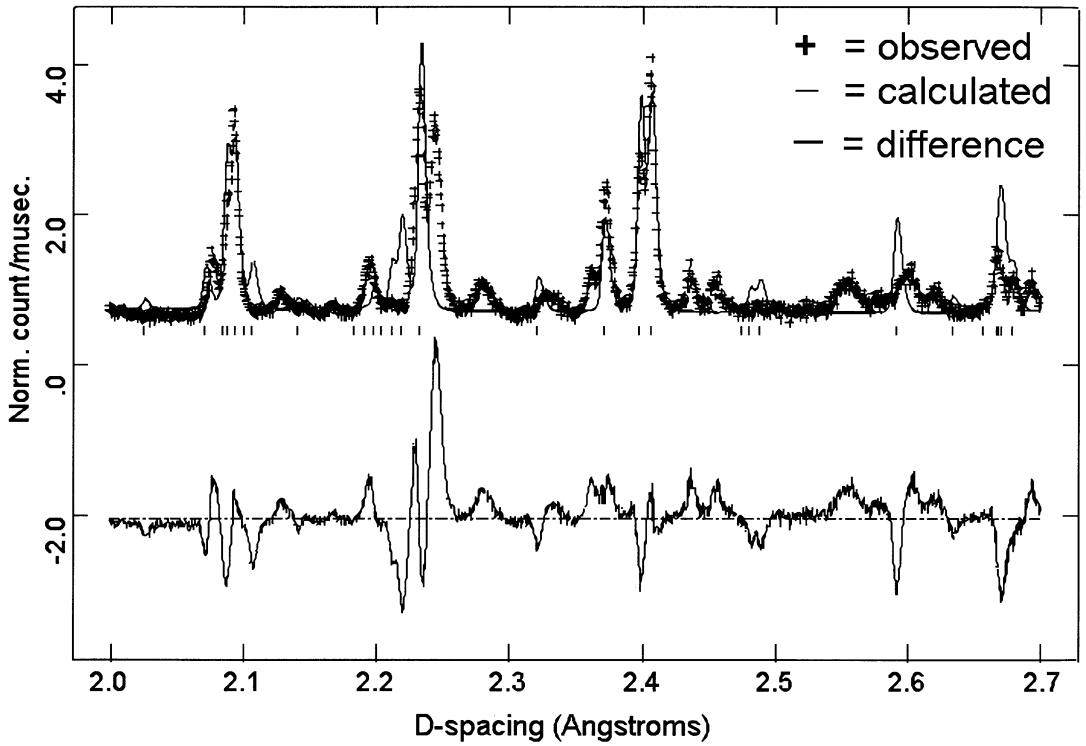

Fig. 5. Rietveld profile fit to synchrotron powder diffraction data from $Sr_2Fe_3O_{6.5-\delta}$ sample. Observed (+), calculated, and difference profiles are shown, along with reflection markers. Note reflection at $d = 2.24$ Å which violates I-centering.

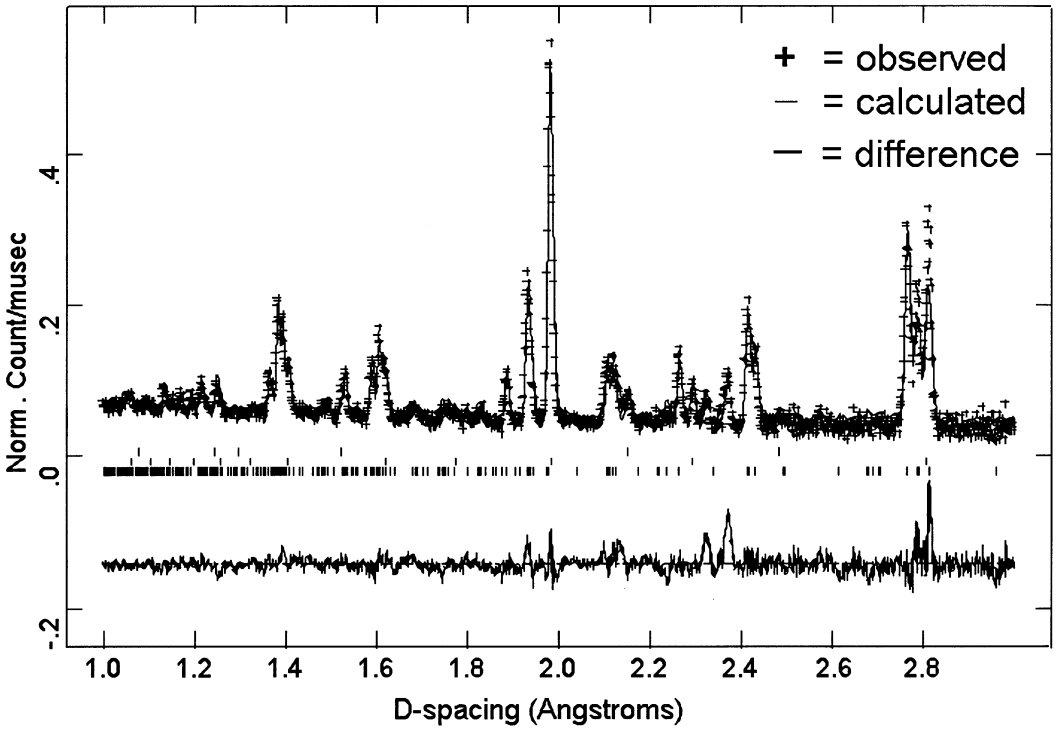

Fig. 6. Rietveld profile fit to ND data of SFC2 sample obtained at 1050 °C in air. Observed, calculated, and difference profiles are shown, along with reflection markers (lowest row: 236 phase; middle row: perovskite; top row: rock salt).

3.2. High temperature diffraction

Fig. 6 shows the observed and calculated patterns obtained from Rietveld refinement of ND SFC2 data (summed over 8 h) at 1050 °C in air. Three phases (236, perovskite and rock salt) are easily identified and the resultant fit is acceptable. Two unassigned reflections at ~2.3 Å are probably from an Fe-rich impurity (presumably an atypical polymorph of Fe_2O_3), that is not evident in ambient temperature data due to strong peak overlap with other phases. The model of Yoshiasa is adequate, although it is not possible to refine oxygen thermal and positional parameters individually in a stable fashion. Positional parameters for oxygen atoms were fixed and thermal parameters constrained together. Thermal parameters for the 5-fold Fe/Co atoms were also constrained.

Unit cell volumes for the 236 and perovskite phases (experiment 2) are plotted versus time in Figs. 7 and 8, respectively, highlighting the dramatically different responses of the two phases to changes in pO_2. The 236 cell volume stabilizes in air at each temperature but shows a continuous increase under Ar, with the rate and magnitude increasing as the temperature is increased. The perovskite phase, on the other hand, shows a rapid and dramatic volume change at all temperatures when cycled between air and Ar, brought about by oxidation and reduction of the Fe/Co and resulting change in oxygen content.

Fractional changes in cell volume, relative to 950 °C in air (plotted versus temperature in Fig. 9), reveal further differences between the 236 and perovskite phases. For both phases at all temperatures the cell volumes are larger in Ar than in air. The magnitudes of increase for the two phases, though, have different trends with increasing temperature. The percentage increase in 236 volume (between air and argon) increases from ~10.13% at 950 °C to ~0.21% at 1050 °C, while corresponding values for perovskite show a decrease from ~1.20% at 950 °C to ~0.96% at 1050 °C. The divergent trend for 236 can be explained by more rapidly decreasing Co and oxygen content in the 236 phase under Ar than under air. In perovskite the difference in oxygen content between the air and Ar measurements at any particular temperature decreases with increasing temperature. This results in the two sets of points showing more of a convergent trend. While the Fe:Co ratios vary for the perovskite in air and Ar at any given temperature, the effect on volume is small.

Fig. 3 (experiment 2 data) shows the weight fraction of each phase in SFC2 as calculated with Rietveld refinement of the individual data sets. At 950 °C in air, the phases are completely stable, but under Ar the 236 phase undergoes partial decomposition into perovskite and rocksalt phases. This decomposition is evident even from visual inspection of the diffraction patterns. The decomposition is readily reversed when switching from Ar to air.

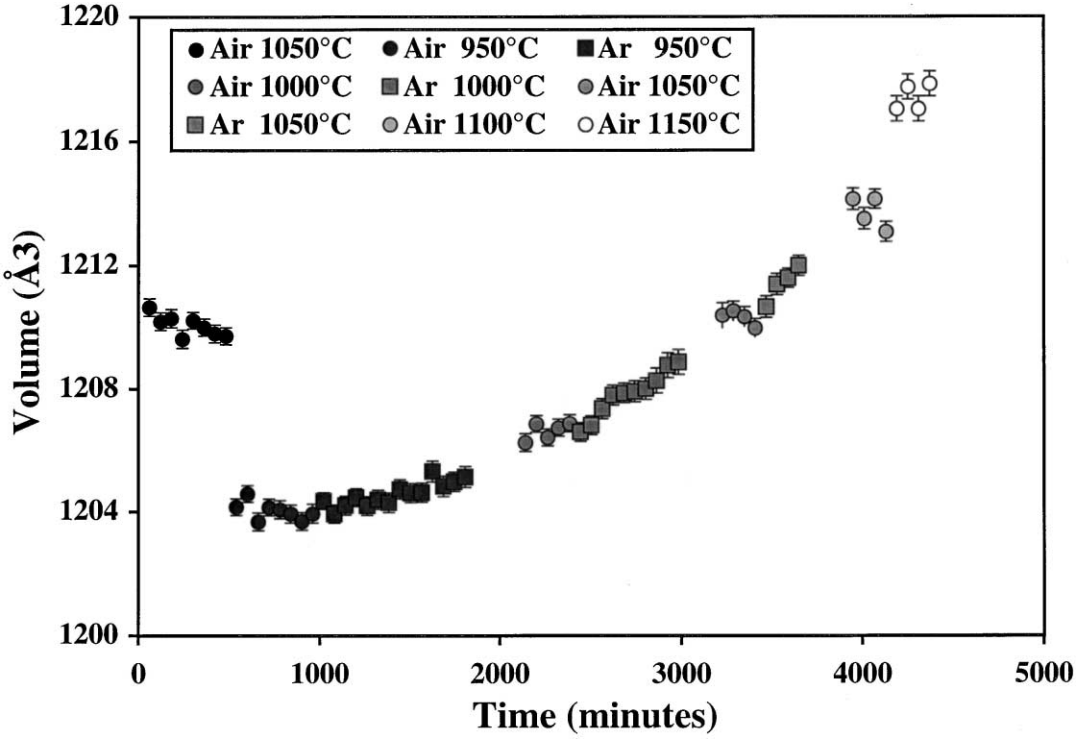

Fig. 7. Cell volume of 236 phase plotted as a function of experimental time over the temperature range of 950–1150 °C in air and Ar.

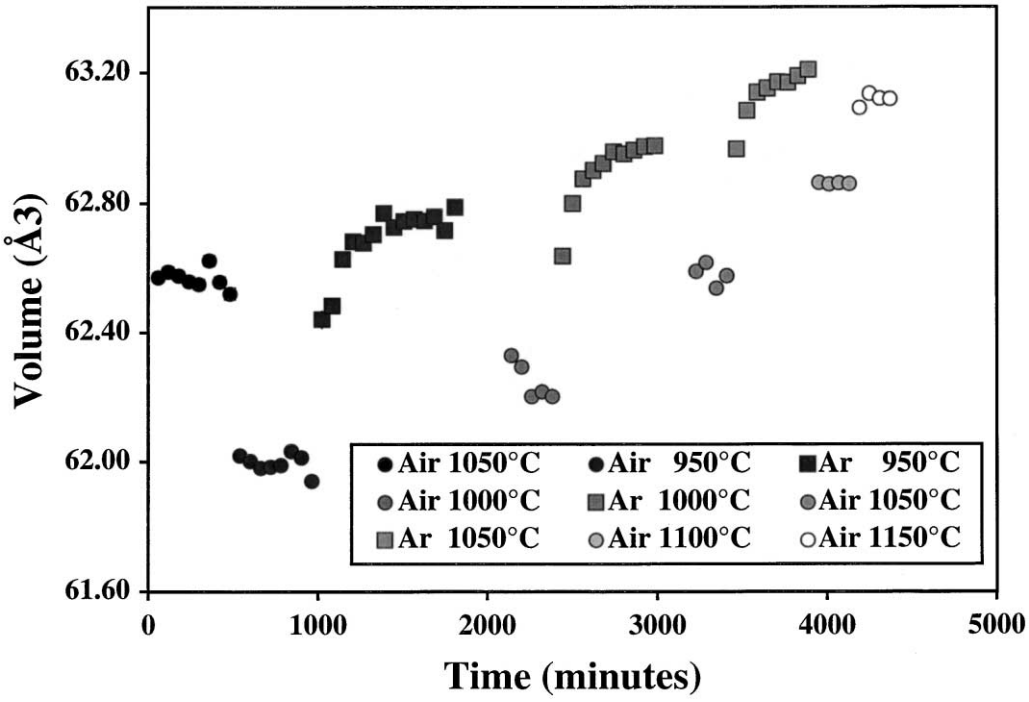

Fig. 8. Cell volume of perovskite phase plotted as a function of experimental time over the temperature range of 950–1150 °C in air and Ar.

"Stabilized" weight fractions for each individual phase from experiments 1–3 are presented in Table 3. The 236 phase content is particularly important, since the physical properties of SFC2 appear to be determined by its presence. Fig. 10 shows how it behaves in air and Ar. The 236 phase content at 1050 °C in air ranges from 68–76% among tubes prepared from various batches of calcined powder. While 236 is stable in air up to 1050 °C, above 1050 °C the 236 phase undergoes a decomposition that accelerates most rapidly

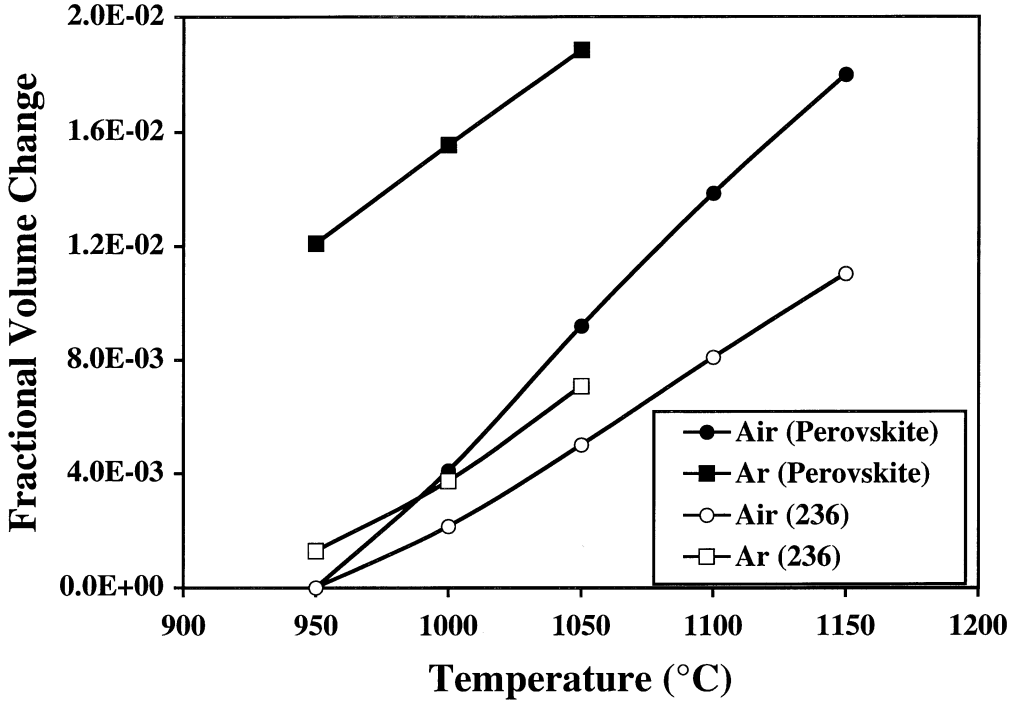

Fig. 9. Fractional changes in unit cell volumes of 236 and perovskite phases, relative to 950 °C in air, plotted as a function of temperature in air and Ar. Data points derived from averages over regions of stability. Open symbols, 236; closed symbols, perovskite.

Table 3
Summary of weight fractions determined for 236, perovskite, and rocksalt phases in SFC2 samples in air and Ar over the temperature range of 900–1200 °C

Experiment	Temperature (°C)	Air			Argon		
		236 (%)	Perovskite (%)	Rock salt (%)	236 (%)	Perovskite (%)	Rocksalt (%)
1	900	74	20	6	73	22	5
2	950	78	16	6	63	27	10
2	1000	80.5	15.5	4	53	35	12
1	1050	69	25	6	–	–	–
2	1050	76.5	18	5.5	38	46	16
2	1050	72	22.5	5.5	–	–	–
3	1050	68	26	6	–	–	–
2	1100	64	25	11	0	–	–
2	1150	55	33	12	0	–	–
3	1200	10	73	17	0	–	–

between 1150 and 1200 °C. The melting point of these samples is ~1240 °C. Our Rietveld analysis indicates that the 236 phase becomes more Fe rich as the decomposition occurs; the perovskite phase also becomes more Fe rich under the same conditions. In an Ar environment (squares in Fig. 10), the situation is different; at 900 °C, there is very little effect on the 236 phase, but at higher temperatures the decomposition occurs rapidly leading to a two-phase system. Again, as decomposition occurs there is an increasing Fe content in the perovskite phase.

It has already been shown that the perovskite phase lattice responds to changes in pO_2. The rapid rate of change is not always clearly evident from the long 60-mm data sets. However, the data collected at 900 °C, shown in Fig. 11, shows that the perovskite phase very rapidly adjusts in when the gas is changed from air to Ar. The first four Ar data points are taken at 15-mm intervals; the following 7 at 30-min intervals. Rapid change occurs over the first 4 h, but this slows and ~7 h are required for the perovskite cell to reach a stable value. When switching from Ar to air, the reverse occurs even more rapidly.

3.3. Perovskite phase vacancy ordering

In experiment 3 (perovskite and rocksalt phases only) the sample was cooled from 1200 to 500 °C. Fig. 12

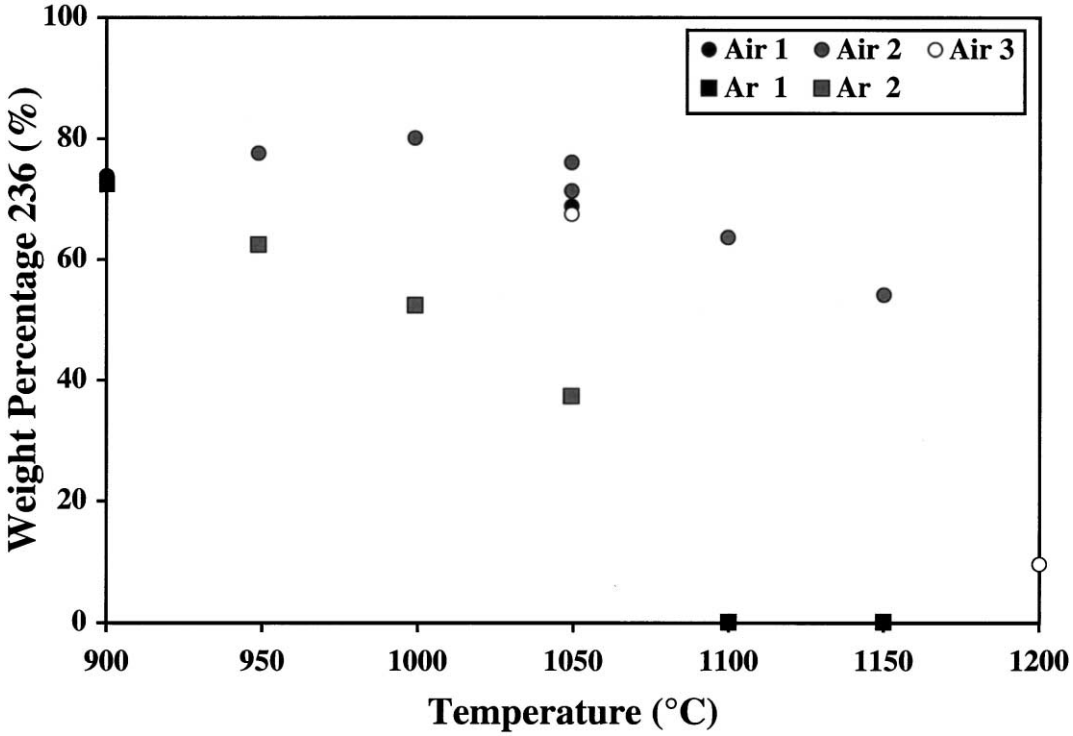

Fig. 10. Weight percentage of 236 phase in SFC2 collected over temperature range of 900–1200 °C under air and Ar (experiments 1–3).

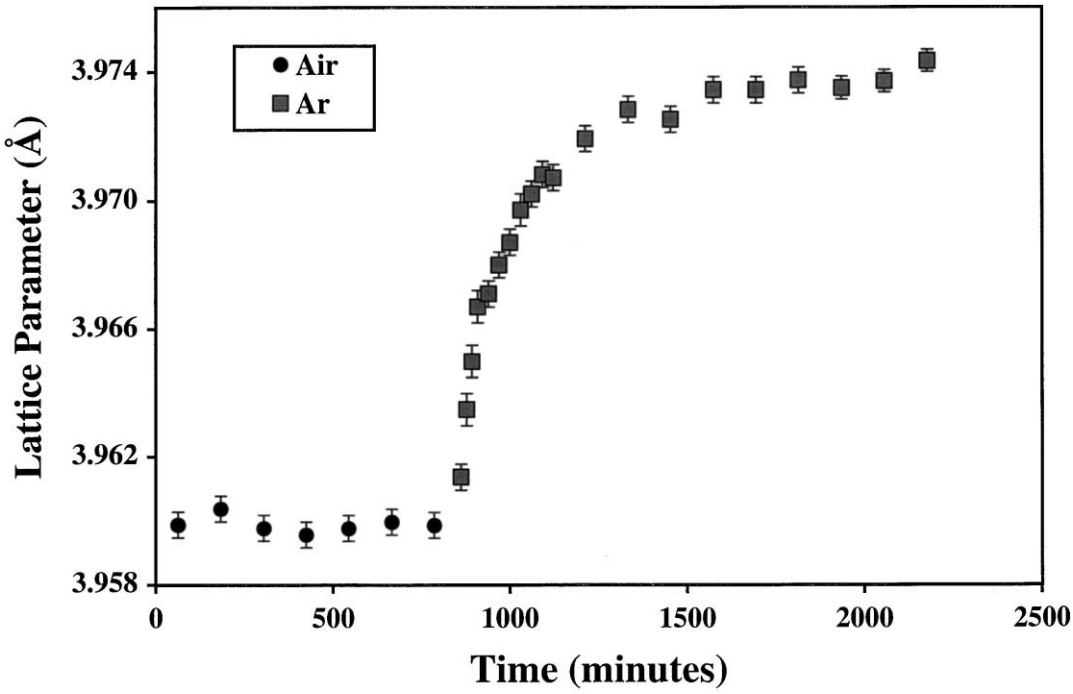

Fig. 11. Unit cell length of perovskite phase in SFC2, collected at 900 °C under air and Ar. Variation in cell parameters controlled by oxygen content of phase.

shows that no ordering of the perovskite phase into brownmillerite occurs until the temperature is below 900 °C. The ordering temperature probably lies in the region of ~850 °C, but the exact temperature would be sample-dependent. At 500 °C, Rietveld refinement indicated that the composition of the brownmillerite phase is $Sr_2Fe_{1.84}Co_{0.16}O_5$, with ~4.5% Co on the tetrahedral and ~12% Co on the octahedral sites. We see no evidence of the formation of a tetragonal phase as noted by Grenier et al.[21] who studied $Sr_2Fe_2O_5$. Liu

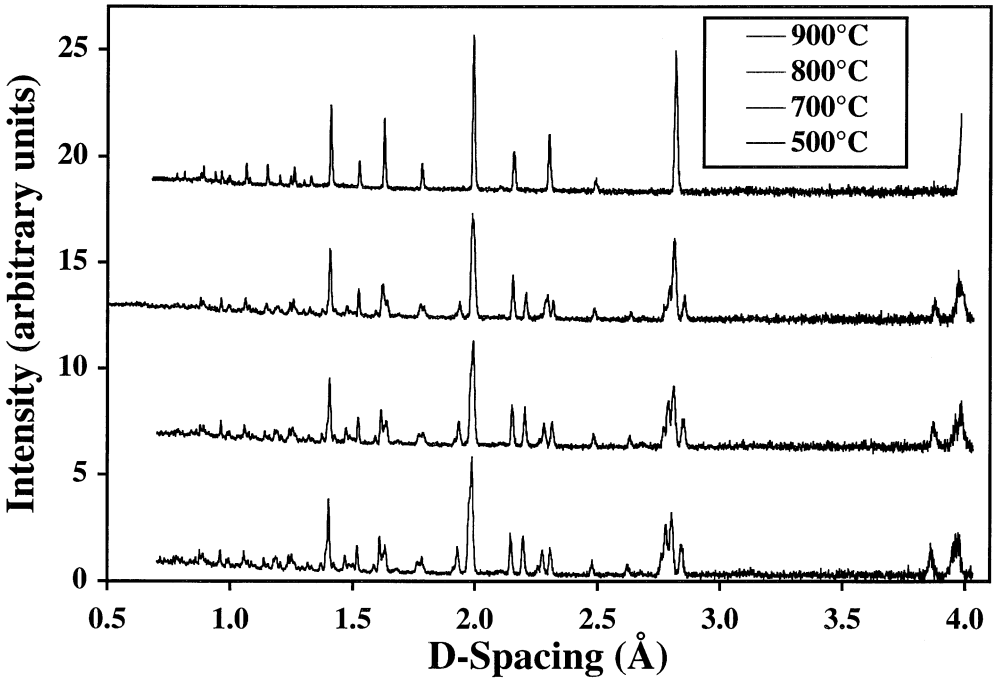

Fig. 12. Vacancy ordering during cooling leads to transformation of perovskite phase into brownmillerite (additional superlattice reflections). From bottom to top, measurements taken at 500, 700, 800 and 900 °C.

et al.[22] report an onset of ordering at ~715 °C during cooling in a thermal gravimetric-differential thermal analysis measurement (N_2) in $SrFe_{0.4}Co_{1.6}O_5$, whereas Kruidhof et al.,[23] from thermogravimetric–differential scanning calorimetry measurements, report an ordering temperature of ~740 °C in the same material.

4. Summary

In situ neutron diffraction experiments on $SrFeCo_{0.5}O_y$ (SFC2) ceramic membrane tubes have studied the phase chemistry of SFC2 under typical synthesis or post annealing conditions. SFC2 is a complex multiphase material that exhibits great change in phase composition depending on conditions. In partially reducing Ar environments and at temperatures above 1050 °C, $Sr_2(Fe,Co)_3O_{6.5-\delta}$ (236) decomposes into the Sr(Fe,Co)$O_{3-\delta}$ perovskite and (Co,Fe)O rocksalt phases, with the extent of decomposition dependent on temperature. Under most circumstances this decomposition is reversible. These condition-dependent changes might well affect the mechanical stability and electrochemical performance of SFC2 membranes when used under operating conditions.

Acknowledgements

The authors gratefully acknowledge the contribution of Dr. D. Cox (National Synchrotron Light Source, Brookhaven National Laboratory) who performed the synchrotron X-ray diffraction measurement. This work is supported by the US Department of Energy, Federal Energy Technology Center and Basic Energy Sciences. This work has benefited from the use of the Intense Pulsed Neutron Source at Argonne National Laboratory. This facility is funded by the US Department of Energy under Contract W-3 1-109-ENG-38.

References

1. Balachandran, U., Dusek, T. J., Sweeney, S. M., Poeppel, R. B., Mieville, R. L., Maiya, P. S., Kleefisch, M. S., Pei, S., Kobylinski, T. P., Udovich, C. A. and Bose, A. C., Methane to syngas via ceramic membranes. *Am. Ceram. Soc. Bull.*, 1995, **74**, 71.
2. Balachandran, U., Dusek, J. T., Maiya, P. S., Mieville, R. L., Ma, B., Kleefisch, M. S. and Udovich, C. A. Separation of gases with solid electrolyte ionic conductors. In *11 th Intersociety Cryogenic Symposium, Energy Week Conference & Exhibition*, 28–30 January 1997. Houston, Texas.
3. Teraoka, Y., Zhang, H. M., Furukawa, S. and Yamazoe, N., Oxygen permeation through perovskite type oxides. *Chem. Lett., 1985, 1743.*
4. Teraoka, Y., Nobunaga, T. and Yamazoe, N., Effect of cation substitution on the oxygen semipermeability of perovskite type oxides. *Chem. Lett., 1988, 503.*
5. Tsai, C. Y., Dixon, A. G., Moser, W. R. and Ma, Y. H., Dense perovskite membrane reactors for partial oxidation of methane to syngas. *Aiche J.*, 1998, **43**, 2741.
6. Kim, S., Yang, Y. L., Christoffersen, R. and Jacobson, A. J., Oxygen permeation, electrical conductivity and stability of the perovskite oxide $La_0.\ 2Sr_{0.8}Cu_{0.4}Co_{0.6}O_{3-x}$. *Solid State Ionics*, 1997, **104**, 57.
7. Qui, L., Lee, T. H., Liu, L. M., Yang, Y. L. and Jacobson, A. J.,

Oxygen permeation studies of $SrCo_{0.8}Fe_{0.2}O_{3-d}$. *Solid State Ionics*, 1998, **76**, 321.
8. Balachandran, U., Dusek, J. T., Mieville, R. L., Poeppel, R. B., Kleefisch, M. S., Pei, S., Kobylinski, T. P., Udovich, C. A. and Bose, A. C., Dense ceramic membranes for partial oxidation of methane to syngas. *Appl. Catal. A: Gen.*, 1995, **133**, 19.
9. Mitchell, B. J., Miller, D. J., Richardson, J. W. Jr., Ma, B. and Hodges, J. P., In-situ neutron diffraction studies of mixed conducting Sr–Fe–Co–O materials. *Mater. Res. Soc. Symp. Proc.*, 1999, **547**, 345.
10. Kim, S., Yang, Y. L., Christoffersen, R. and Jacobson, A. J., Determination of oxygen permeation kinetics in a ceramic membrane based on the composition $SrFeCo_{0.5}O_{3.25-d}$. *Solid State Ionics, 1998, 109–187*.
11. Guggilla, S. and Manthiram, A., Crystal chemical characterization of the mixed conductor $Sr(Fe,Co)_{1.50}O_y$. *J. Electrochem. Soc.*, 1997, **144**, L120.
12. Ma, B., Hodges, J. P., Jorgensen, J. D., Miller, D. J., Richardson, J. W., Jr. and Balachandran, U., Structure and property relationships in mixed-conducting $Sr_4(Fe_{1-x}Co_x)_6O_{13\pm d}$. *J. Solid State Chem.*, 1998, **141**, 576.
13. Von-Harder, H. and Müller-Buschbaum, H. K., Darstellung und untersuchung von $Sr_2Fe_2O_5$-einkristallen em betrag zur kristallchemie von $M_2Fe_2O_5$-verbindungen. *Z. Anorg. Allg. Chem.*, 1980, **464**, 169.
14. Greaves, C., Jacobson, A. J., Tofield, B. C. and Fender, B. E. F., A powder neutron diffraction investigation of the nuclear and magnetic structure of $Sr_2Fe_2O_5$. *Acta Crystallogr.*, 1975, **B31**, 641.
15. Harrison, W. T. A., Lee, T. H., Yang, Y. L., Scarfe, D. P., Liu, L. M. and Jacobson, A. J., A neutron diffraction study of two strontium cobalt iron oxides. *Mater. Res. Bull.*, 1995, **30**, 621.
16. Battle, P. D., Gibb, T. C. and Lightfoot, P., The crystal and magnetic structures of Sr_2CoFeO_5. *J. Solid State Chem.*, 1988, **76**, 334.
17. Larson, A.C. and Dreele, R.B.V. Generalized structure analysis system (GSAS). Los Alamos National Laboratory LA-UR-86-748 (1987).
18. Asti, G., Carbucicchio, M., Deriu, A., Lucchini, E. and Sloccari, G., Magnetic properties and spin order of $Sr_7Fe_{10}O_{22}$. *J. Magn. Magn. Mater.*, 1978, **8**, 65.
19. Yoshiasa, A., Ueno, K., Kanamuru, F. and Horiuchi, H., Structure of $Sr_4Fe_6O_{13}$ a new perovskite-derivative in the Sr–Fe–O system. *Mater. Res. Bull.*, 1986, **21**, 175.
20. Fjellvåg, H., Hauback, B. C. and Bredsen, R., Crystal structure of the mixed conductor $Sr_4Fe_4Co_2O_{13}$. *J. Mater. Chem.*, 1997, **7**, 2415.
21. Grenier, J.-C., Ea, N., Pouchard, M. and Hagenmuller, P., Structural transitions at high temperature in $Sr_2Fe_2O_5$. *J. Solid State Chem.*, 1985, **58**, 243.
22. Liu, L. M., Lee, T. H., Qui, L., Yang, Y. L. and Jacobson, A. J., A thermogravimetnc study of the phase diagram of strontium cobalt iron oxide, $SrCo_{0.8}Fe_{0.2}O_{3-d}$. *Mater. Res. Bull.*, 1996, **31**, 29.
23. Kruidhof, H., Bouwmeester, H. J. M., Doom, R. H. E. v. and Burggraaf, A. J., Influence of order–disorder transitions on oxygen permeability through selected nonstoichiometric perovskite-type oxides. *Solid State Ionics*, 1993, **63**, 816.